



# Hydrodynamical wind on vertically self-gravitating ADAFs in the presence of toroidal magnetic field

Maryam Ghasemnezhad<sup>1</sup>★ and Shahram Abbassi<sup>2,3</sup>★

<sup>1</sup>Faculty of physics, Shahid Bahonar University of Kerman, Kerman, Iran

<sup>2</sup>Department of Physics, School of Sciences, Ferdowsi University of Mashhad, Mashhad, 91775-1436, Iran

<sup>3</sup>School of Astronomy, Institute for Research in Fundamental Sciences (IPM), Tehran, 19395-5531, Iran

Accepted 2015 November 5. Received 2015 November 4; in original form 2014 December 4

## ABSTRACT

We present the effect of a hydrodynamical wind on the structure and the surface temperature of a vertically self-gravitating magnetized advection-dominated accretion flows (ADAFs) using self-similar solutions. Also a model for an axisymmetric, steady-state, vertically self-gravitating hot accretion flow threaded by a toroidal magnetic field has been formulated. The model is based on  $\alpha$ -prescription for turbulence viscosity. It is found that the thickness and radial velocity of the disc are reduced significantly as wind gets stronger. In particular, the solutions indicated that the wind and advection have the same effects on the structure of the disc. We also find that the thin ADAF becomes hotter by including the wind parameter and the self-gravity parameter.

**Key words:** accretion, accretion discs – black hole physics – magnetic fields – MHD – stars: black holes – stars: winds, outflows.

## 1 INTRODUCTION

The accretion of matter into a compact object is a classical problem in modern astrophysics and is an important tool for understanding energetic phenomena including active galactic nuclei (AGN), ultraluminous X-ray sources and galactic jets. The standard theory of astrophysical accretion disc was formulated over 30 years ago (Pringle & Rees 1972; Novikov & Thorne 1973; Shakura & Sunyaev 1973; Kato, Fukue & Mineshige 2008). An accretion disc is a structure formed by diffuse material in spiral motion around a massive central body by losing their initial angular momentum and some of the gravitational energy which liberate and convert into radiation.

The accretion disc theory has been developed rapidly during the past three decades. Since then a large body of observational data has been accumulated; however, required some other types of models distinct from the classical picture. Advective cooling is one of the most important mechanisms which are not considered in the energy equations in the standard model. In another point of view, if the gas density is low, the gas maybe unable to radiate energy at a rate that balances viscous heating. In this case, the heat generated by viscosity will be advected inwards with the flow instead of being radiated. The disc becomes hot, hence geometrically thick, low density, and radiatively inefficient. Such advection-dominated accretion flows (ADAFs) were introduced by Narayan & Yi (1994). In comparison to thin accretion discs, advection-dominated flows

have quite different structure, lower bolometric efficiency, and very different spectral energy distributions, with emission over a wider range of wavelengths. It has been argued (Yuan & Narayan 2014, a comprehensive review and reference there in), based on a combination of theoretical models and observational studies of stellar mass black holes, that the inner regions of accretion discs are replaced by ADAFs when the accretion rate decreases below  $\sim 0.01\dot{M}_{\text{Edd}}$ . The dynamical and radiative properties of the ADAFs have been intensely studied during the past several years. Consequently, the model has been applied to astrophysical black hole systems, such as supermassive black hole in our Galactic Centre, Sagittarius A\* (Sgr A\*), low-luminosity AGNs (LLAGNs), and black hole binaries in their hard and quiescence states. Although ADAF works well for Sgr A\* and some LLAGNs, many details of ADAF need to be investigated (e.g. the dynamical role of magnetic field, the influence of outflow, etc.). In order to deepen our understanding of the accretion process modelling to more sources is required.

The importance and presence of magnetic fields in the accretion discs are generally accepted. The dynamical importance of magnetic field is widely recognized in angular-momentum transport, the formation of jets outflow, and the interactions between holes and discs, etc. Several attempts have been done for studying magnetized accretion flows analytically (Kaburaki 2000; Akizuki & Fukue 2006; Abbassi, Ghanbari & Najjar 2008; Abbassi, Ghanbari & Ghasemnezhad 2010; Ghasemnezhad, Khajavi & Abbassi 2012). More or less, they confirmed that in the presence of a magnetic field, the structure and dynamics of the flow will change considerably. Therefore, it is apparently essential to develop ADAFs model for a fully magnetized case. On the other hand, observations and theoretical arguments show that hot accretion flows are associated

\* E-mail: [m\\_ghasemnezhad2005@yahoo.com](mailto:m_ghasemnezhad2005@yahoo.com) (MG); [abbassi@um.ac.ir](mailto:abbassi@um.ac.ir) (SA)

with outflow (Blandford & Begelman 1999). A physically more satisfactory approach had been proposed by Akizuki & Fukue (2006), Abbassi et al. (2008, 2010), and Ghasemnezhad, Khajavi & Abbassi (2013) by adding outflow and wind effects on the radial structure of ADAFs.

In the pioneer ADAFs paper, the effect of self-gravity in the vertical (or even in radial direction) is completely neglected for simplicity and assumed that the disc is supported in the vertical direction only by the thermal pressure. Mosallanezhad et al. (2012) studied the vertical self-gravitating ADAFs in the presence of toroidal magnetic field. Their solutions showed the thickness of the disc modified significantly when self-gravity becomes stronger. In this paper, we develop Mosallanezhad et al. (2012) solutions by considering the effect of wind in the magnetohydrodynamic (MHD) equations. The hypothesis of the model and relevant equations are developed in Section 2. Self-similar solutions are presented in Section 3. We show the result in Section 4 and finally we present the summary and conclusion in Section 5.

## 2 THE BASIC EQUATIONS

Our goal here is to study the effect of wind on the magnetized ADAF in the presence of the vertical self-gravity of the disc. We ignored the self-gravity in radial direction. We used vertically integrated MHD equations in cylindrical coordinates  $(r, \varphi, z)$  for steady-state and axisymmetric ( $\frac{\partial}{\partial \varphi} = \frac{\partial}{\partial t} = 0$ ) hot accretion disc. we suppose that all flow variables are only a function of  $r$  (radial direction). We ignore the relativistic effects and we use Newtonian gravity in the radial direction. We suppose that the gaseous disc is rotating around a compact object of mass  $M_*$ . By adopting  $\alpha$ -prescription for viscosity of rotating gas in accretion flow, we consider that the magnetic field has just toroidal component.

The equation of continuity gives

$$\frac{\partial}{\partial r}(r\Sigma V_r) + \frac{1}{2\pi} \frac{\partial \dot{M}_w}{\partial r} = 0, \quad (1)$$

where  $V_r$  is the accretion velocity ( $V_r < 0$ ) and  $\Sigma = 2\rho H$  is the surface density at a cylindrical radius  $r$ .  $H$  is the disc half-thickness and  $\rho$  is the density. Mass-loss rate by wind is showed by  $\dot{M}_w$ . Therefore,

$$\dot{M}_w = \int 4\pi r' \dot{m}_w(r') dr', \quad (2)$$

where  $\dot{m}_w(r)$  is the mass-loss per unit area from each disc face. On the other hand, we can rewrite the continuity equation as

$$\frac{1}{r} \frac{\partial}{\partial r}(r\Sigma V_r) = 2\dot{\rho}H, \quad (3)$$

where  $\dot{\rho}$  is the mass-loss rate per unit volume. The equation of motion in the radial direction is

$$V_r \frac{\partial V_r}{\partial r} = \frac{V_\varphi^2}{r} - \frac{GM_*}{r^2} - \frac{1}{\Sigma} \frac{d}{dr} (\Sigma c_s^2) - \frac{c_A^2}{r} - \frac{1}{2\Sigma} \frac{d}{dr} (\Sigma c_A^2), \quad (4)$$

where  $V_\varphi$ ,  $G$ ,  $c_s$ , and  $c_A$  are the rotational velocity of the flow, the gravitational constant, sound speed, and Alfvén velocity of the gas, respectively. The sound speed and the Alfvén velocity are defined as  $c_s^2 = \frac{p_{\text{gas}}}{\rho}$  and  $c_A^2 = \frac{B_\varphi^2}{4\pi\rho} = \frac{2p_{\text{mag}}}{\rho}$ , where  $B_\varphi$ ,  $p_{\text{gas}}$ , and  $p_{\text{mag}}$  are the toroidal component of magnetic field, the gas, and magnetic pressure, respectively.

By integrating along  $z$  of the azimuthal equation of motion gives

$$r\Sigma V_r \frac{d}{dr}(rV_\varphi) = \frac{d}{dr} \left( r^3 \nu \Sigma \frac{d\Omega}{dr} \right) - \frac{\Omega(lr)^2}{2\pi} \frac{d\dot{M}_w}{dr}, \quad (5)$$

where  $\nu$  is the kinematic viscosity coefficient.  $\alpha$ -prescription (Shakura & Sunyaev 1973) for viscosity was assumed as

$$\nu = \alpha c_s H, \quad (6)$$

where  $\alpha$  is a constant less than unity.  $\Omega (= \frac{V_\varphi}{r})$  is the angular speed. To write the angular momentum equation, we have considered the role of wind in transferring the angular momentum. It is assumed that the wind material moving along a stream line originating at radius  $r$  in the disc and corotate with the disc out to a radial distance  $lr$ . The wind material ejected at radius  $r$  on the disc and carries away specific angular momentum  $(lr)^2\Omega$ , where  $\Omega$  is related to a radial distance  $lr$ . Knigge (1999) defines the  $l$  parameter as the length of the rotational lever arm that allows us to have many types of accretion disc winds models. The parameter  $l = 0$  corresponds to a non-rotating wind and the angular momentum is not extracted by the wind and the disc losses only mass because of the wind, while  $l \neq 1$  represents outflowing materials that carry away the angular momentum (Knigge 1999; Abbassi, Nourbakhsh & Shadmehri 2013).

By integrating along  $z$  of the hydrostatic balance, we have

$$H = \frac{c_s^2(1+\beta)}{2\pi G \Sigma}, \quad (7)$$

where  $\beta = \frac{p_{\text{mag}}}{p_{\text{gas}}} = \frac{1}{2} \left( \frac{c_A}{c_s} \right)^2$  indicates the importance of magnetic field pressure compared to gas pressure. We will study the dynamical properties of the disc for different values of  $\beta$ .

Here, we consider only self-gravity in the vertical direction, and assume that in the radial direction, centrifugal forces are balanced by gravity from a central mass (Keplerian approximation). One can estimate the importance of self-gravity of the disc by comparing the contributions to the local gravitational acceleration in the vertical direction by both the central object and the disc itself. Hereafter, we will often refer to such accretion discs, in which self-gravity is important only in the vertical direction, as Keplerian self-gravitating discs (Duschl, Strittmatter & Biermann 2000). The vertical gravitation due to the disc's self-gravity at the disc surface is given by  $(2\pi G \Sigma)$ , and due to the central object is given by  $\frac{GM_* H}{r^3}$ . Thus, self-gravity of the disc in vertical direction is dominated if (Mosallanezhad et al. 2012)

$$2\pi G \Sigma > \frac{GM_* H}{r^3} \quad (8)$$

$$\frac{M_d}{M_*} > \frac{1}{2} \frac{H}{r}, \quad (9)$$

where  $M_d(r) = \pi r^2 \Sigma$  is the mass enclosed in the disc within a radius  $r$ .

For increasing disc masses self-gravity first becomes important in the vertical direction. Since the enclosed mass,  $M_d$ , is an increasing function of the radial distance,  $r$ , the effect of vertical self-gravity becomes progressively important in outer part of the disc, especially in thick discs (for ADAFs the typical value of  $H/r$  is around 1).

On the other hand in a self-gravitating disc, the hydrostatic equilibrium equation in the vertical direction yields (e.g. Paczynski 1978; Duschl, Strittmatter & Biermann 2000)

$$P = \pi G \Sigma^2, \quad (10)$$

where  $P$  is the pressure in  $z = 0$  (central plane). Following Mosallanezhad et al. (2012), we assume the disc to be isothermal in the vertical direction.

In order to complete the problem, we need to introduce energy equation. We assume the generated energy due to viscous dissipation into the volume is balanced by the advection cooling and energy loss of outflow. Thus,

$$\frac{\Sigma V_r}{\gamma - 1} \frac{dc_s^2}{dr} - 2H V_r c_s^2 \frac{d\rho}{dr} = f \Sigma \nu r^2 \left( \frac{d\Omega}{dr} \right)^2 - \frac{1}{2} \eta \dot{m}_w(r) V_k^2(r), \quad (11)$$

where  $\gamma$ ,  $f$ , and  $\Omega_k$  are adiabatic index, the ratio of specific advection parameter and the Keplerian angular speed, respectively. The last term on the right-hand side of the energy equation represents the energy loss due to wind or outflow (Knigge 1999). In our model,  $\eta$  is a free and dimensionless parameter. The large  $\eta$  corresponds to more energy extraction from the disc because of wind (Knigge 1999). Finally since we consider the toroidal configuration magnetic field, the induction equation can be written as

$$\frac{d}{dr}(V_r B_\phi) = \dot{B}_\phi, \quad (12)$$

where  $\dot{B}_\phi$  is the field escaping/creating rate due to magnetic instability or dynamo effect.

### 3 SELF-SIMILAR SOLUTIONS

In the last section, we introduced the basic equations for a vertically self-gravitating, axisymmetric, magnetized hot accretion flow in the presence of rotating wind. The basic equations of the model are a set of partial differential equations, which have a very complicated structure. The self-similar method is one of the most useful and powerful techniques to give an approximate solutions for differential MHD equations and has a wide range of applications in astrophysics. For the first time, this technique was applied by Narayan & Yi (1994) in order to solve ADAFs dynamical equations. By adopting Narayan & Yi (1994) self-similar scaling, in fact, the radial dependences of all physical quantities are cancelled out, and all of differential equations are transformed to algebraic equations. Using self-similar scaling and including the effect of mass outflow and making the reasonable assumption as introduced by Abbassi et al. (2010) and Mosallanezhad et al. (2012), the velocities are supposed to be expressed as follows,

$$V_r(r) = -c_1 \alpha V_k(r) \quad (13)$$

$$V_\phi(r) = c_2 V_k(r) \quad (14)$$

$$c_s^2 = c_3 V_k^2 \quad (15)$$

$$c_A^2 = 2\beta c_s^2, \quad (16)$$

where

$$V_k(r) = \sqrt{\frac{GM}{r}}. \quad (17)$$

Generally,  $c_1$ ,  $c_2$ , and  $c_3$  possess radial dependences. But we will show in Fig. 1 that their slopes with respect to radius are small over the range of radii considered ( $r > 30r_s$ ). The deviations will be small as well, and that the strongest deviations occur at the smallest radii. As it is clear  $c_1$ ,  $c_2$ , and  $c_3$  are almost constant in the range of  $r = 30r_s$  to  $r = 100r_s$ . This is the most accepted range

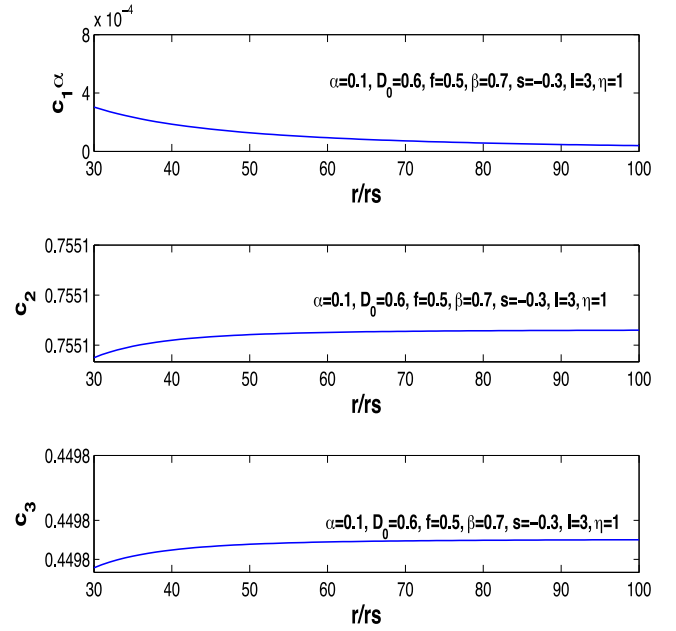


**Figure 1.** Numerical coefficient  $c_i$  as function of radius. This range is most accepted radial range for ADAFs for a given values of input parameters.

for validity of advection-dominated discs. On the other hand, the self-similar solutions that we had been adopted are valid far from the boundaries. It is clear that in the main body of the disc where the self-similar assumption is valid,  $c_i$  are almost constant. Hereafter, we used constant  $c_1$ ,  $c_2$ , and  $c_3$  and they are determined later from the basic equations. Assuming the surface density ( $\Sigma$ ) to be in the form of

$$\Sigma = \Sigma_0 r^s, \quad (18)$$

where  $s$  is constant. In order to have a valid solution for the self-similar treatment, the mass-loss rate per unit volume and the field escaping rate must have the following form:

$$\dot{\rho} = \dot{\rho}_0 r^{2s-1/2} \quad (19)$$

$$\dot{B}_\phi = \dot{B}_0 r^{s-3/2}. \quad (20)$$

Considering hydrostatic equation, we obtain the disc half-thickness  $H$  as

$$H = \frac{c_3(1+\beta)}{2 \frac{M_d}{M_*}} r = \frac{c_3(1+\beta)}{D} r,$$

$D (= 2 \frac{M_d}{M_*})$  is dimensionless parameter and represents the importance of vertical self-gravitation of the disc. By substituting the above self-similar solutions in to the dynamical equations of the system, we obtain the following system of dimensionless equations, to be solved for  $c_1$ ,  $c_2$ , and  $c_3$ :

$$\dot{\rho}_0 = - \left( s + \frac{1}{2} \right) \frac{c_1 \alpha \pi (\Sigma_0)^2 \sqrt{GM_*}}{2c_3(1+\beta)M_*} \quad (21)$$

$$H = \frac{c_3(1+\beta)M_*}{2\pi\Sigma_0} r^{-s-1}. \quad (22)$$

By using equations (1), (2), and (3) we have

$$\dot{M}_w = \dot{M}_{0w} r^{s+1/2}, \quad (23)$$

where

$$\dot{M}_{0w} = 2\pi\alpha c_1 \sqrt{GM_*} \Sigma_0 \quad (24)$$

$$\dot{m}_w = \frac{s+1/2}{2} \alpha c_1 \sqrt{GM_* \Sigma_0} r^{s-3/2}, \quad (25)$$

we define  $\dot{m}$  as

$$\dot{m} = \frac{\dot{M}_{0w}}{\pi \alpha \Sigma_0 \sqrt{GM_*}}, \quad (26)$$

therefore,

$$\dot{m} = 2c_1. \quad (27)$$

Equations (28)–(31) come from equations (4), (5), (11), and (12), respectively:

$$-\frac{1}{2} c_1^2 \alpha^2 = c_2^2 - 1 - [s - 1 + \beta(s + 1)] c_3 \quad (28)$$

$$c_1 = \frac{-3(1+\beta)}{D} c_3^{3/2} + \dot{m} \left( s + \frac{1}{2} \right) l^2 \quad (29)$$

$$\left[ \frac{1}{\gamma - 1} + (2s + 1) \right] c_1 c_3 = \frac{9}{4D} f c_3^{3/2} c_2^2 (1 + \beta) - \frac{1}{8} \eta \left( s + \frac{1}{2} \right) \dot{m} \quad (30)$$

$$\dot{B}_0 = \frac{(1-2s)}{2} \alpha \Sigma_0 c_1 G \sqrt{M_*} \sqrt{\frac{2\beta}{1+\beta}}. \quad (31)$$

As it is easily seen from equation (21), for  $s = -1/2$ , there is no mass-loss/wind, while there exists mass-loss (wind) for  $s > -1/2$ . On the other hand, the escape/creation of magnetic fields will balance each other for  $s = 1/2$  (equation 31). In this work, we focus on the wind case ( $-1/2 < s < 1/2$ ). Furthermore, the thickness of the disc will increase due to the magnetic pressure for the weakly-to-moderately magnetized flow with  $\beta \sim 1$ ; while it decreases when  $D$  is relatively large.

After algebraic manipulations, we obtain a sixth-order algebraic equation for  $c_1$ :

$$A^3 c_1^6 - 3(1-E) A^2 c_1^4 + [B^3 + 3A(1-E)^2] c_1^2 - (1-E)^3 = 0, \quad (32)$$

where

$$A = \frac{1}{2} \alpha^2 \quad (33)$$

$$B = \frac{4}{3^{5/3} f} \left[ \frac{1}{\gamma - 1} + (2s + 1) \right] \left( \frac{D}{1 + \beta} \right)^{2/3} \left[ \frac{1}{-1 + 2 \left( s + \frac{1}{2} \right) l^2} \right] - [s - 1 + \beta(s + 1)] \left[ \frac{D}{3(1 + \beta)} \left( -1 + 2 \left( s + \frac{1}{2} \right) l^2 \right) \right]^{2/3} \quad (34)$$

$$E = \frac{\eta}{3f} \left[ \frac{s + \frac{1}{2}}{-1 + 2 \left( s + \frac{1}{2} \right) l^2} \right]. \quad (35)$$

Mosallanezhad et al. (2012) solved the equation when  $s = -1/2$  because they did not consider wind/mass-loss in their model. But we are interested in analysing the dynamical behaviour of magnetized ADAFs in the presence of mass-loss. This algebraic equation shows that the variable  $c_1$  which determines the behaviour of radial velocity depends only on the  $\alpha$ ,  $s$ ,  $D$ ,  $\beta$ , and  $f$ . As we can see in above equations, in order to have the real solutions for  $c_1$ , we need to have  $l$  as  $l^2 > \frac{1}{2s+1}$ . This new requirement limits the solutions of

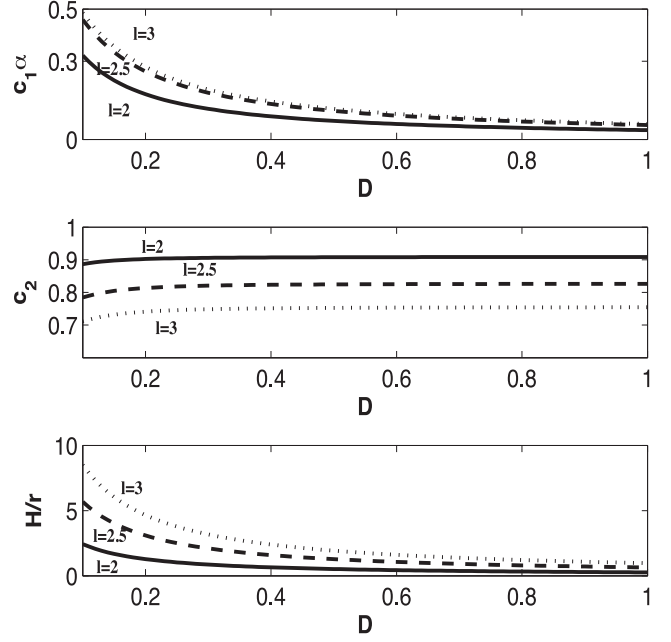


**Figure 2.** Numerical coefficient  $c_i$  as function of self-gravity parameter  $D$  for several values of  $l$  (the amount of the extracted angular momentum). For all panels, we use  $s = -0.3$ ,  $\beta = 0.7$ ,  $\alpha = 0.1$ ,  $\eta = 1$ , and  $f = 0.5$ .

$c_3 > 0$ . Using  $c_1$  from this algebraic equation, the other variables (i.e.  $c_2$  and  $c_3$ ) can be obtained easily:

$$c_2^2 = \frac{4Dc_3^{-1/2}c_1}{9f(1+\beta)} \left[ \frac{1}{\gamma - 1} + (2s + 1) \right] + \frac{\eta \left( s + \frac{1}{2} \right) Dc_1c_3^{-3/2}}{9f(1+\beta)} \quad (36)$$

$$c_3 = c_1^{2/3} \left[ \frac{D \left( -1 + 2 \left( s + \frac{1}{2} \right) l^2 \right)}{3(1+\beta)} \right]^{2/3}. \quad (37)$$

We can solve these simple equations numerically, and clearly just physical solutions can be interpreted. They reduce to the results of Mosallanezhad et al. (2012) without wind. Now we can analyse the behaviour of solutions.

## 4 RESULTS

Now, we have performed a parameter study considering our input parameters. We are interested to examine the effects of rotating wind, magnetic field, self-gravity, and advection for which their characteristic parameters are  $s$ ,  $l$ ,  $\beta$ ,  $D$ , and  $f$ , respectively. We solved the equations of  $c_i$  numerically. According to the new condition for  $l$ , we use  $l > 1$  to obtain real values for  $c_1$ ,  $c_2$ , and  $c_3$ .  $l > 1$  corresponds to rotating wind which can remove a significant amounts of angular momentum from the disc. Our results for the structure of vertically self-gravitating hot magnetized ADAFs are shown in Figs 2–6. In all these figures, the necessary constant are fixed to their most typical values. In all the figures, we use  $\gamma = 5/3$ . Fig. 2 shows the coefficients  $c_1$ ,  $c_2$ , and  $H/r$  in terms of self-gravitating parameter  $D$  for different values of dimensionless lever arm  $l$  ( $l = 2, 2.5, 3$ ). In Fig. 2, we investigate the role of the extraction of angular momentum due to the wind/outflow in the radial velocity, rotation velocity and the thickness of accretion flow. The behaviour of radial velocity is determined by  $c_1 \alpha$  as shown in the upper panel. Top panel in Fig. 2 shows that for larger values of parameter  $D$ , which implies self-gravitating becomes

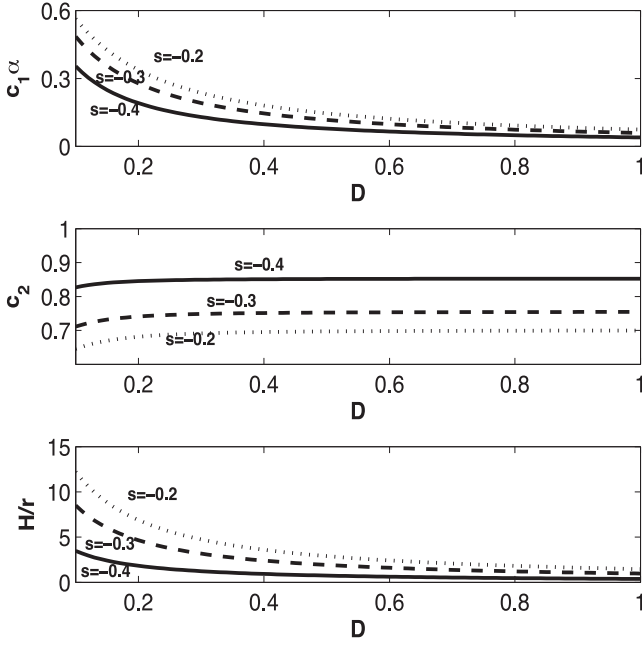
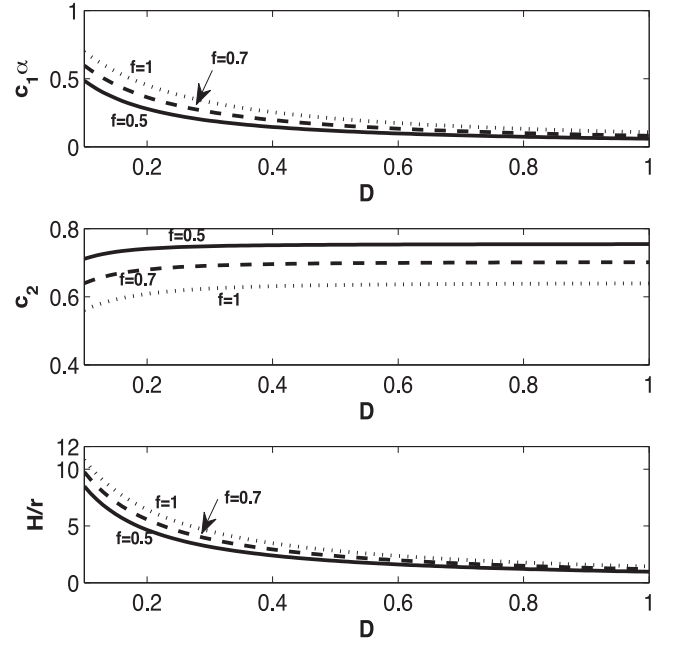


**Figure 3.** Numerical coefficient  $c_i$  as function of self-gravity parameter  $D$  for several values of  $s$  (wind parameter). For all panels, we use  $l = 3$ ,  $\beta = 0.7$ ,  $\alpha = 0.1$ ,  $\eta = 1$ , and  $f = 0.5$ .

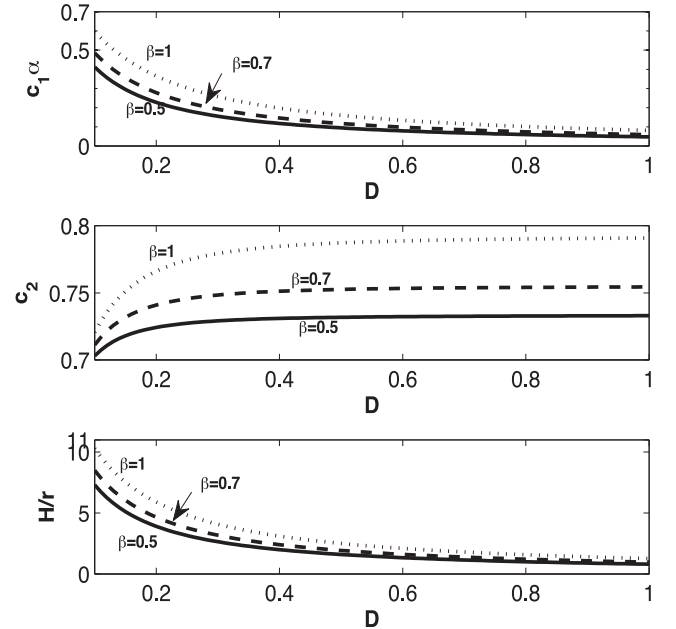
important, the radial velocity decreases sharply as parameter  $D$  increases. Furthermore, when  $l$  becomes stronger the radial velocity steadily increases which makes sense and is in great agreement with Abbassi et al. (2013). The rotational velocity,  $c_2$ , is plotted in the middle panel. As we can see easily, the rotational velocity is almost independent of the self-gravity parameter  $D$ . Abbassi et al. (2013) have shown that the accreting flow will rotate slower when the angular momentum removal from the disc, as  $l$  becomes larger. This trend is observed in our results (middle panel of Fig. 2). Bottom panel of Fig. 2 shows the relative thickness of disc,  $H/r$  as a function of  $D$  for different values of  $l$  parameter. For instance, one would immediately deduce that the relative thickness decreases meaningfully at the outer part of the disc, where the disc becomes self-gravitating (larger values of  $D$ ). On the other hand for non-self-gravitating discs, small  $D$ , the half-thickness increases when the amount of the extracted angular momentum becomes stronger. These results agree with previous solution (Abbassi et al. 2013). In Fig. 2, each curve is labelled by corresponding index  $l$ .

Fig. 3 shows the coefficients  $c_1$ ,  $c_2$ , and  $H/r$  in terms of self-gravitating parameter  $D$  for different values of wind parameter  $s$ . For lower values of  $D$ , non-self-gravitating case, the radial velocity increases when the wind becomes stronger, which is in agreement with Abbassi et al. (2013). The rotational velocity is almost independent of the self-gravity parameter  $D$ , middle panel. We increase the wind parameter, we see rotational velocity decreases. The relative thickness of disc,  $H/r$ , decreases gradually at the outer part of the disc, where the disc becomes self-gravitating (larger values of  $D$ ). Also for non-self-gravitating discs, lower  $D$ , the half-thickness increases when the wind is stronger ( $s > -1/2$ ). These results agree with previous solutions (Mosallanezhad et al. 2012; Abbassi et al. 2013). In Fig. 2, each curve is labelled by corresponding index  $s$ .

In Fig. 4, the behaviour of the coefficients  $c_1$  and  $c_2$  and relative thickness are shown for different values of advective parameter  $f$  versus parameter  $D$ . As disc becomes advective, larger  $f$ , the radial velocity and half-thickness will increase relatively, while the rota-



**Figure 4.** Numerical coefficient  $c_i$  as function of self-gravity parameter  $D$  for several values of  $f$  (advection parameter). For all panels, we use  $s = -0.3$ ,  $\beta = 0.7$ ,  $\alpha = 0.1$ ,  $\eta = 1$ , and  $l = 3$ .



**Figure 5.** Numerical coefficient  $c_i$  as function of self-gravity parameter  $D$  for several values of  $\beta$  (magnetic field parameter). For all panels we use  $s = -0.3$ ,  $f = 0.5$ ,  $\alpha = 0.1$ ,  $\eta = 1$ , and  $l = 3$ .

tional velocity decreases, particularly for smaller values of  $D$ . The rotational velocity decreases when advective parameter  $f$  increases and is not affected by the self-gravity parameter. But radial velocity and vertical thickness are sensitive to  $D$  parameter and decrease as  $D$  increases.

Similar to Figs 2, 3, and 4, the coefficients  $c_1$  and  $c_2$  and relative thickness are shown in Fig. 5 for different values of magnetic parameter  $\beta$  versus parameter  $D$ . Generally, when the magnetic field becomes stronger, when the  $\beta$  increases, the flow rotate faster with

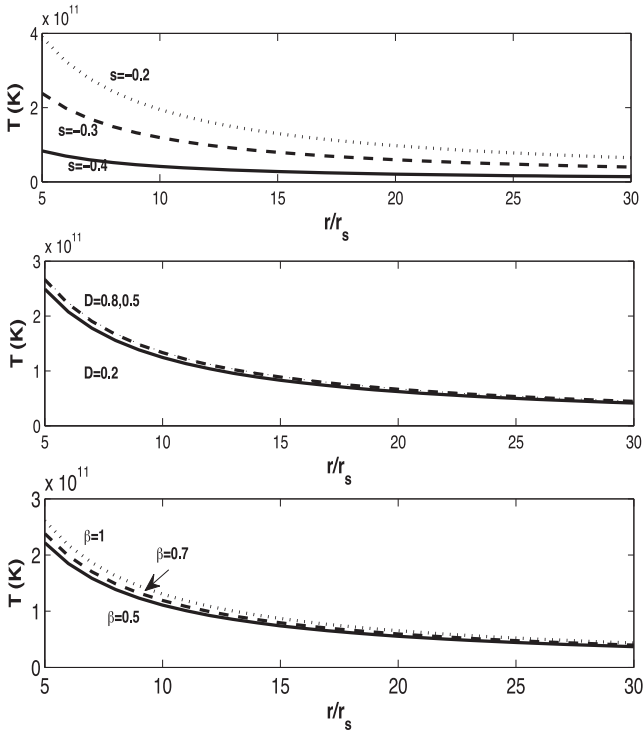


**Figure 6.** This plot shows the surface temperature of the disc  $T(k)$  as function of dimensionless radius ( $r/r_s$ ) for several values of top panel: wind parameter ( $s$ ), middle panel: self-gravity parameter  $D$  and bottom panel: magnetic field parameter ( $\beta$ ). Numerical coefficient  $c_i$  as function of self-gravity parameter  $D$  for several values of  $f$  (advection parameter). For all panels we use  $\eta = 1$ .

much more radial velocity and larger half-thickness compare to non-magnetized case. It would be interesting if we study the influence of the input parameters on the temperature gradient of the disc. Finally, in Fig. 6, we have shown the influence of the wind (upper panel), self-gravity (middle panel) and the magnetic field (lower panel) on the radial temperature structure of the flow. As we know, ADAFs occur in two regimes depending on their mass accretion rate and optical depth. In the limit of low mass accretion rates, we have optically thin discs. In optically thin ADAFs, the cooling time of accretion flow is longer than the accretion time-scale. The generated heat by viscosity remains mostly in the accretion disc. The disc cannot radiate their energy efficiently. In this model, we may estimate the isothermal sound speed as (Akizuki & Fukue 2006)

$$\frac{R}{\bar{\mu}} T = c_s^2 = c_3 \frac{GM_*}{r}, \quad (38)$$

where  $T$  is the gas temperature,  $R$  is the gas constant and  $\bar{\mu}$  is the mean molecular weight ( $\bar{\mu} = 0.5$ ). So, the temperature is expressed as

$$T = c_3 \frac{c^2 \bar{\mu}}{2R} \left( \frac{r}{r_s} \right)^{-1} = 2.706 \times 10^{12} c_3 \left( \frac{r}{r_s} \right)^{-1}, \quad (39)$$

where  $r_s (= 2 \frac{GM_*}{c^2})$  and  $c$  are the Schwarzschild radius of the central object and light speed, respectively. In this formula, the coefficient  $c_3$  implicitly depends on the wind, self-gravitation, magnetic field, and advection parameters, ( $s, D, \beta, f$ ). In Fig. 5, we show the radial behaviour of temperature for different value of  $s, D$ , and  $\beta$ . It is obvious that the surface temperature decreases monotonically as  $r/r_s$  increases. As we can see in the top panel of Fig. 6, for the case of strong wind ( $s > -0.5$ ), the surface temperature of the disc will

increase significantly, at least in the inner part of the disc, and this can impact the observed spectrum since most observed luminosity of ADAFs comes from inner most region.

In the lower panel of Fig. 6, we will see the effect of the magnetic field parameter,  $\beta$ , on the surface temperature of disc. The surface temperature increases by increasing  $\beta$ . Finally in the lower panel, we have plotted the surface temperature for several values of the self-gravity parameter  $D$ . Temperature gradient of the disc is not very sensitive to the value of  $D$ , while though  $\beta$  and  $s$  more significant effect are observed. Also it is not easy to calculate the radiative spectrum of optically thin ADAFs. This model of ADAFs do not radiate away like a blackbody radiation. Since accreting gas in a hot accretion flow has a very high temperature and is moreover optically thin and magnetized, the relevant radiation processes are synchrotron emission and bremsstrahlung, modified by Comptonization (Yuan & Narayan 2014). In the other limit, the optically thick ADAFs or slim disc, the mass accretion rate and the optical depth is very high. So the radiation generated by accretion disc can be trapped within the disc. In optically thick ADAFs, the radiation pressure dominates and sound speed is related to radiation pressure. This model radiates away locally like a blackbody radiation. The averaged flux  $F$  is

$$\Pi = \Pi_{\text{rad}} = \frac{1}{3} a T_c^4 2H = \frac{8H}{3c} \sigma T_c^4 \quad (40)$$

$$F = \sigma T_c^4 = \frac{3c}{8H} \Pi = \frac{3}{8} c \Sigma_0 \frac{D}{1+\beta} GM r^{s-2}, \quad (41)$$

where  $\Pi$ ,  $T_c$ , and  $\sigma$  is the height-integrated gas pressure, the disc central temperature, and the Stefan–Boltzmann constant, respectively. The optical thickness of the disc in the vertical direction is

$$\tau = \frac{1}{2} \kappa \Sigma = \frac{1}{2} \kappa \Sigma_0 r^s, \quad (42)$$

where  $\kappa$  is the electron-scattering opacity. Therefore, the effective temperature of the disc surface becomes

$$\sigma T_{\text{eff}}^4 = \frac{\sigma T_c^4}{\tau} = \frac{3c}{4\kappa} \frac{D}{1+\beta} \frac{GM}{r^2} = \frac{3}{4} \frac{D}{1+\beta} \frac{L_E}{4\pi r^2} \quad (43)$$

$$T_{\text{eff}} = \left[ \frac{3L_E}{16\pi\sigma} \frac{D}{(1+\beta)} \right]^{1/4} r^{-1/2}, \quad (44)$$

where  $L_E = 4\pi c \frac{GM}{\kappa}$  is the Eddington luminosity. As we can see, there is no  $f$  and  $s$  dependence in the surface temperature of the optically thick ADAFs. The surface temperature is influenced by the self-gravity and magnetic field parameters explicitly. It is clear that the temperature increases by adding  $D$  parameter and decreases for larger values of the magnetic field ( $\beta$ ). In the self-gravitating optically thick ADAFs, the surface temperature is not affected by wind parameter.

## 5 SUMMARY AND CONCLUSION

In this paper, we have studied the accretion disc around black hole in an advection-dominated regime in the presence of a toroidal magnetic field and vertical self-gravity of the disc. It was assumed that disc wind/outflow contributes to loss of mass, angular momentum, and thermal energy from accretion discs. We used the self-similar method for solving the equations. Although the self-similar solutions are too simple, they improve our understanding of the physics

of the accretion discs around black hole. For simplicity, we assume an axially symmetric and static flow with  $\alpha$ -prescription of viscosity. Also we ignore the relativistic effects and we use Newtonian gravity in the radial direction. We consider the vertical self-gravity of disc by following the paper of Mosallanezhad et al. (2012) in the presence of the effect of wind. Our results reproduce their solutions when the effect of wind is neglected. In ADAFs, the more dissipated energy is advected in the flow and therefore, ADAFs are hot and thick. The disc rotates slower and becomes thicker in the presence of strong rotating wind. Also we have shown the self-gravity and wind parameter have the opposite effects on the thickness and radial velocity of the disc. The rotational velocity almost is not sensitive to the self-gravity while it has a more significant effect to the wind parameter. Beside we have shown the self-gravity and wind parameter have the same effects on the surface temperature in the optically thin ADAFs.

### ACKNOWLEDGEMENTS

The authors thank the anonymous referee for the careful reading of the manuscript and his/her insightful and constructive comments. SA acknowledges the support from the Abdus Salam International Centre for Theoretical Physics (AS-ICTP) for his visit through the regular associateship scheme.

### REFERENCES

- Abbassi S., Ghanbari J., Najjar S., 2008, MNRAS, 388, 663  
 Abbassi S., Ghanbari J., Ghasemnezhad M., 2010, MNRAS, 409, 1113  
 Abbassi S., Nourbakhsh E., Shadmehri M., 2013, ApJ, 765, 96  
 Akizuki C., Fukue J., 2006, PASJ, 58, 469  
 Blandford R. D., Begelman M. C., 1999, MNRAS, 303, 1  
 Duschl W., Strittmatter P. A., Biermann P. L., 2000, A&A, 357, 1123  
 Ghasemnezhad M., Khajavi M., Abbassi S., 2012, ApJ, 750, 57  
 Ghasemnezhad M., Khajavi M., Abbassi S., 2013, Ap&SS, 346, 341  
 Kaburaki O., 2000, ApJ, 531, 210  
 Kato S., Fukue J., Mineshige S., 2008, Black Hole Accretion Discs. Kyoto Univ. Press, Kyoto  
 Knigge C., 1999, MNRAS, 309, 409  
 Mosallanezhad A., Abbassi S., Shadmehri M., Ghanbari J., 2012, Ap&SS, 337, 703  
 Narayan R., Yi I., 1994, ApJ, 428, L13  
 Novikov I. D., Thorne K. S., 1973, in Dewitt C., Dewitt B. S., eds, Black Holes (Les Astres Occlus). Gordon & Breach, New York, p. 343  
 Paczynski B., 1978, Acta Astron., 28, 91  
 Pringle J. E., Rees M. J., 1972, A&A, 21, 1  
 Shakura N. I., Sunyaev R. A., 1973, A&A, 24, 337  
 Yuan F., Narayan R., 2014, ARA&A, 52, 529

This paper has been typeset from a  $\text{\TeX}/\text{\LaTeX}$  file prepared by the author.